Resolvin D1 binds human phagocytes with evidence for proresolving receptors

Resolvin D1 binds human phagocytes with evidence for proresolving receptors

Sriram Krishnamoorthy[a,1], Antonio Recchiuti[a,1], Nan Chiang[a], Stephanie Yacoubian[a], Chih-Hao Lee[b], Rong Yang[a], Nicos A. Petasis[c], and Charles N. Serhan[a,2]

[a]Center for Experimental Therapeutics and Reperfusion Injury, Department of Anesthesiology, Perioperative, and Pain Medicine, Brigham and Women's Hospital and Harvard Medical School, Boston, MA 02115; [b]Department of Genetics and Complex Diseases, Harvard University School of Public Health, Boston, MA 02115; and [c]Department of Chemistry, Loker Hydrocarbon Institute, University of Southern California, Los Angeles, CA 90089

Edited by Charles A. Dinarello, University of Colorado Denver, Aurora, CO, and approved December 3, 2009 (received for review July 2, 2009)

Endogenous mechanisms that act in the resolution of acute inflammation are essential for host defense and the return to homeostasis. Resolvin D1 (RvD1), biosynthesized during resolution, displays potent and stereoselective anti-inflammatory actions, such as limiting neutrophil infiltration and proresolving actions. Here, we demonstrate that RvD1 actions on human polymorphonuclear leukocytes (PMNs) are pertussis toxin sensitive, decrease actin polymerization, and block LTB_4-regulated adhesion molecules (β2 integrins). Synthetic [^{3}H]-RvD1 was prepared, which revealed specific RvD1 recognition sites on human leukocytes. Screening systems to identify receptors for RvD1 gave two candidates—ALX, a lipoxin A_4 receptor, and GPR32, an orphan—that were confirmed using a β-arrestin-based ligand receptor system. Nuclear receptors including retinoid X receptor-α and peroxisome proliferator-activated receptor-α, -δ, -γ were not activated by either resolvin E1 or RvD1 at bioactive nanomolar concentrations. RvD1 enhanced macrophage phagocytosis of zymosan and apoptotic PMNs, which increased with overexpression of human ALX and GPR32 and decreased with selective knockdown of these G-protein-coupled receptors. Also, ALX and GPR32 surface expression in human monocytes was up-regulated by zymosan and granulocyte-monocyte–colony-stimulating factor. These results indicate that RvD1 specifically interacts with both ALX and GPR32 on phagocytes and suggest that each plays a role in resolving acute inflammation.

inflammation | leukocytes | lipid mediators | resolution | polyunsaturated fatty acids

Acute inflammation is a tightly controlled protective host response where chemical mediators such as prostaglandins and leukotrienes play pivotal roles that are signaled via G-protein-coupled receptors (GPCRs) (1). Excessive inflammation has emerged as a critical component in many prevalent human diseases such as atherosclerosis and cancer (2, 3). Therefore, endogenous control mechanisms in inflammation are of interest. It is now recognized that resolution of acute inflammation is an active and highly regulated process, which involves endogenous anti-inflammatory pathways stopping excessive infiltration of neutrophils [polymorphonuclear leukocytes (PMNs)], as well as proresolution circuits aimed at clearing apoptotic PMNs from a site [for a recent review, see ref. 4]. Local mediators orchestrating anti-inflammation and resolution act via GPCRs (4). For example, lipoxin A_4, a potent anti-inflammatory and proresolving mediator, binds to its receptor ALX (5), which stops further PMN recruitment and activates nonphlogistic phagocytosis of apoptotic PMNs (6).

Within the immune system, dietary supplementation with eicosapentaenoic acid and docosahexaenoic acid has many reported beneficial actions (7). A systems approach with self-resolving inflammatory exudates using mediator lipidomics–informatics, proteomics, and analysis of cellular trafficking led to the identification of resolvins and protectins (4). These mediator families are derived from ω-3 fatty acids and are part of a recently described genus of anti-inflammatory and proresolving autacoids with potent actions in experimentally induced animal diseases [(8); reviewed in refs. 7 and 9)]. At least two GPCRs are involved in transducing resolvin E1 (RvE1) signals, namely ChemR23 and BLT1 (10, 11).

Resolvin D1 (RvD1) biosynthesis and structure were established (8) and its stereochemistry assigned 7*S*, 8*R*, 17*S*-trihydroxy-4*Z*, 9*E*, 11*E*, 13*Z*, 15*E*, and 19*Z*-docosahexaenoic acid (12). RvD1 limits PMN infiltration at nanogram levels in murine peritonitis and blocks transendothelial migration of human PMNs (8, 12) as well as enhances phagocytosis by human macrophages (MΦ) (13). Recently, RvD1 was found to directly act at a single-cell level in microfluidic chambers to stop human PMN migration to interleukin-8 (14). Here, we prepare synthetic [^{3}H]-RvD1 and present evidence for specific RvD1 surface recognition on human leukocytes and identification of two GPCRs.

Results

RvD1 Regulates Actin Polymerization: Pertussis Toxin Sensitivity. Because RvD1 directly acts on human PMNs (14), we tested whether it can regulate actin polymerization, a key event in neutrophil migration (15). Human PMNs incubated with RvD1 (10 nM) resulted in a decrease in actin polymerization (Fig. 1*A*), which was evident within 5 min in a time-dependent fashion (Fig. S1). To assess whether GPCRs are involved in RvD1 signal transduction, PMNs were treated with either pertussis toxin (PTX) or activated cholera toxin (see *Materials and Methods*) and then incubated with RvD1. As shown in Fig.1*A*, PTX treatment diminished the RvD1-dependent block in actin polymerization, whereas incubation with activated cholera toxin did not affect this response, suggesting that RvD1 acts via a PTX-sensitive GPCR. Exposure of PMNs to RvD1 (10 nM) significantly blocked LTB_4 (10 nM)-stimulated actin reorganization (Fig. 1*B*) and significantly decreased LTB_4 (10 nM) up-regulated cell-surface expression of the integrin CD11b (Fig. 1*C*). Interestingly, RvD1 did not stimulate intracellular Ca^{2+} mobilization (Fig. 1*D*) or activate cAMP with human PMNs ($n = 3$ healthy subjects; Fig. S2), suggesting that these classic second messengers are not activated by RvD1 signaling in these cells.

Author contributions: S.K., A.R., N.C., and C.N.S. designed research; S.K., A.R., N.C., S.Y., C.-H.L., and R.Y. performed research; R.Y. and N.A.P. contributed new reagents/analytic tools; S.K., A.R., N.C., S.Y., C.-H.L., R.Y., and C.N.S. analyzed data; S.K., A.R., N.C., and C.N.S. wrote the paper; and C.N.S. conceived overall research plan.

Conflict of interest statement: Resolvins are biotemplates for stable analogs. Patents on these are awarded and assigned to the Brigham and Women's Hospital, and C.N.S. is the inventor. These analog patents are licensed for clinical development. All other authors have no conflict of interest.

This article is a PNAS Direct Submission.

[1]S.K. and A.R. contributed equally to this work.

[2]To whom correspondence should be addressed at: Brigham and Women's Hospital/Harvard Medical School, 77 Avenue Louis Pasteur, HIM 829, Boston, MA 02115. E-mail: cnserhan@zeus.bwh.harvard.edu.

This article contains supporting information online at www.pnas.org/cgi/content/full/0907342107/DCSupplemental.

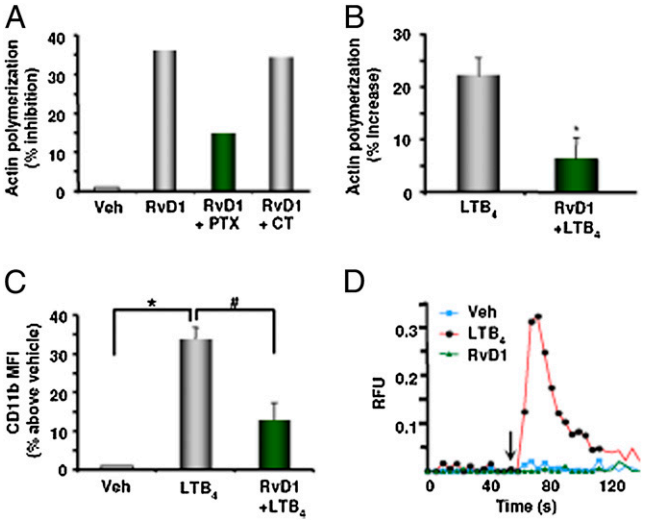

Fig. 1. RvD1 counter-regulates LTB_4 actions with human leukocytes. (*A*) Actin polymerization in PMNs incubated with RvD1 (10 nM) alone (15 min at 37 °C) or following treatment with PTX or cholera toxin for 2 h. (*B*) Actin polymerization in PMNs incubated with LTB_4 (10 nM, 10 sec) alone or with RvD1 (10 nM) followed by LTB_4 (10 nM). (*, $P < 0.05$ compared to LTB_4). (*C*) CD11b surface expression with PMNs incubated with LTB_4 (10 nM, 15 min) alone or with RvD1 (10 nM) followed by LTB_4 (10 nM) (*, $P < 0.05$ vs. vehicle alone; #, $P < 0.05$ vs. LTB_4; MFI, mean fluorescence intensity). (*D*) RvD1 (10 nM) does not mobilize intracellular Ca^{2+} in PMNs compared to LTB_4 (10 nM). Arrow denotes time intervals (RFU, relative fluorescence intensity). Results in *A* and *D* are representative of three healthy subjects. (*B* and *C*) Means ± SEMs from three healthy subjects.

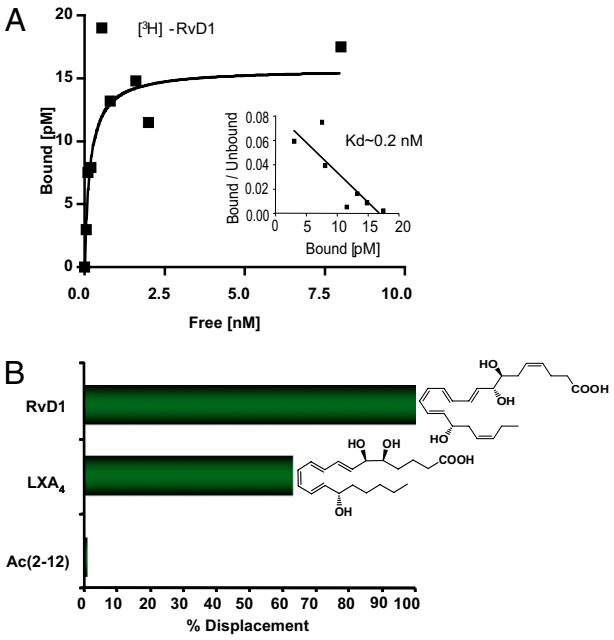

Fig. 2. [^{3}H]-RvD1 specific binding to human leukocytes. (*A*) Saturation curve and Scatchard plot (*inset*) obtained with PMNs incubated with indicated concentrations of [^{3}H]-RvD1 in the presence or absence of 3 log orders excess of unlabeled RvD1. (*B*) Competition binding of [^{3}H]-RvD1 with homoligand RvD1 and heteroligands LXA_4 or Annexin (Ac2-12) peptide. Results are the percentage displacement of [^{3}H]-RvD1-specific binding. Results in *A* are representative of $n = 4$ and in *B* are the mean of triplicate determinations with healthy subjects.

RvD1 Does Not Activate Nuclear Receptors. Nuclear receptors may evoke anti-inflammatory responses (16). Therefore, we sought to determine whether RvD1 interacts with specific nuclear receptors. To this end, HEK-293 cells were cotransfected with constructs of ligand-binding domains from a panel of nuclear receptors linked to a Gal4 DNA-binding domain, along with a Gal4-responsive luciferase reporter. In this system, RvD1 did not directly activate mouse peroxisome proliferator-activated receptor (PPAR)-α, -γ, and -δ or human retinoid X receptor-α (Fig. S3). These results indicated that RvD1 in its anti-inflammatory dose range (9) did not activate these specific nuclear receptors nor did RvE1 (Fig. S3).

[^{3}H]-RvD1-Specific Binding. We next determined whether human leukocytes display specific RvD1-binding sites. To this end, tritium-labeled resolvin D1 ([^{3}H]-RvD1) was prepared by catalytic hydrogenation of synthetic [13, 14]-acetylenic RvD1 methyl ester (Fig. S4). Following catalytic hydrogenation with tritium, ^{3}H-labeled RvD1 coeluted with authentic RvD1 methyl ester beneath a single HPLC peak and gave the characteristic UV absorbance maximum at 301 nm with shoulders at 280 and 315 nm (8, 12). Next, [^{3}H]-RvD1 methyl ester was subjected to saponification to obtain the corresponding carboxylic acid, [13,14]-[^{3}H]-RvD1, which was isolated immediately before each binding experiment ($n = 8$). Representative saturation curves and Scatchard analysis are shown in Fig. 2*A*. These results indicate that [^{3}H]-RvD1 specifically binds to human leukocytes with high affinity ($K_d = 0.17 \pm 0.06$ nM; representative of four healthy subjects). Competition binding was performed with RvD1, LXA_4, and the annexin 1-derived peptide Ac2-12, an anti-inflammatory peptide ligand that binds to ALX (17). The homoligand RvD1 displaced [^{3}H]-RvD1 binding to cells, and the extent of displacement was taken as 100% specific binding. This specific binding was partially displaced by LXA_4 (~60%) whereas the peptide Ac2-12 did not compete (Fig. 2*B*). In parallel, [^{3}H]-RvD1 also displayed specific binding with human monocytes (Fig. S5). These results demonstrated the high affinity and specific binding of RvD1.

Screening for RvD1 Receptor Candidates. Because the handling of [^{3}H]-RvD1 is not without difficulties, we sought functional screening systems that do not rely on labeled ligand. To this end, and because RvD1 counters the actions of TNF-α (8), a luciferase-based reporter system used for identification of the RvE1 receptor ChemR23 (10) was employed for initial screening. This system used a luciferase-based reporter that measures NF-κB activity in response to TNF-α (Fig. 3, *left inset*). cDNA sequences of phylogenetically related GPCRs were cloned into pcDNA3 vector and then cotransfected into HeLa cells together with a reporter vector consisting of NF-κB promoter sequence linked to the luciferase gene. This panel of phylogenetically related receptors was chosen for screening because of their functions related to inflammation, e.g., chemoattraction (1). Among these GPCRs, RvD1 significantly reduced the TNF-α-stimulated NF-κB response in cells overexpressing either ALX or the orphan, GPR32 (Fig. 3). In contrast, cells transfected with other phylogenetically related GPCRs (Fig. 3, *right*), including BLT1, BLT2, CB1, GPR-1, FPR, and ChemR23 [see *Materials and Methods* for National Center for Biotechnology Information (NCBI) accession numbers], did not significantly inhibit TNF-α-stimulated NF-κB luciferase activity on addition of RvD1.

RvD1 Directly Acts at GPR32 and ALX. To monitor RvD1 receptor–ligand interactions, we used a GPCR–β-arrestin–coupled system (Fig. 4*A*) (18) because RvD1 did not evoke Ca^{2+} mobilization (Fig. 1). Incubation of GPR32–β-arrestin cells with RvD1 gave a dose-dependent increase in the interactions of β-arrestin and the receptor in these cells, EC_{50}, of ~8.8×10^{-12} M (Fig. 4*B*). In parallel, incubations with LXA_4 also led to a dose-dependent increase in the activation of GPR32 (EC_{50} ~3.4×10^{-11} M) (Fig.

PHARMACOLOGY

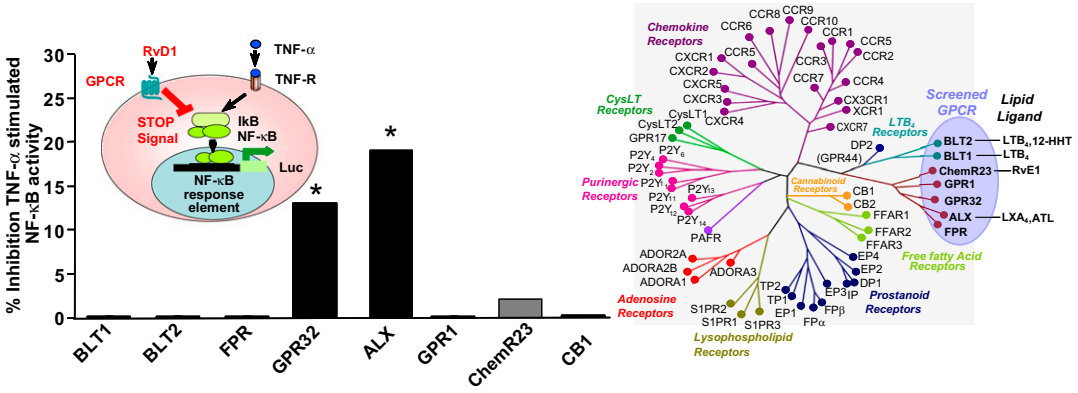

Fig. 3. Screening of RvD1 GPCR candidates. (*Left*) Inhibition of NF-κB activity in HeLa cells overexpressing GPCRs (see text for accession numbers) treated with RvD1 (10 nM, 30 min) followed by TNF-α (1 ng) for 6 h. Values were subtracted from those obtained with mock transfected cells ($n = 6$; *, $P < 0.05$ compared with BLT2, assigned as negative control). (*Inset*) The screening system (see text for details). (*Right*) Radial phylogenetic tree for GPCR protein sequences. GPCRs screened as putative RvD1 receptors are in boldface type, and the cluster generated with ClustalW2 (www.ebi.ac.uk/Tools/clustalw2) is based on deduced amino acid sequences in the NCBI database and constructed with TreeIllustrator software (www.genohm.com). ATL, aspirin-triggered lipoxin; 12-HHT, 12S-hydroxy-5Z,8E,10E-heptadecatrienoic acid (33).

4*C*). These findings indicate that RvD1 and LXA_4 each directly activated GPR32. Recently, nitrosylated pyrazolone derivatives that have agonistic activity with the ALX receptor were described. Among these, a C-5 substituent with an isopropyl group, denoted compound 43, exhibited anti-inflammatory properties, potently inhibiting PMN migration and markedly reducing mouse ear inflammation (19).

As a known ALX anti-inflammatory agonist, compound 43 was tested with the β-arrestin system stably expressing GPR32. Interestingly, compound 43 activated GPR32 ($EC_{50} = 2.25 \times 10^{-12}$ M; Fig. 4*D*). In contrast, side-by-side comparisons indicated that RvD1 did not evoke interaction of β-arrestin with ChemR23 compared to its lipid mediator ligand (10) RvE1 ($EC_{50} \sim 1.3 \times 10^{-11}$ M; Fig. 4*E*), demonstrating high selectivity of these ligands for interacting with these specific GPCRs. RvD1 directly activated ALX with an affinity of $EC_{50} \sim 1.2 \times 10^{-12}$ M, which is comparable to LXA_4 ($EC_{50} \sim 1.1 \times 10^{-12}$ M; Fig. 4 *F* and *G*). An ALX receptor antagonist *tert*-butoxycarbonyl (*t*-Boc) Met-Leu-Phe peptide (20) blocked receptor activation by RvD1 and LXA_4 ($IC_{50} \sim 10^{-5}$ M; Fig. 4 *F* and *G*, *insets*), thus providing evidence for specific interactions of these ligands with ALX. Again, using compound 43 with ALX stable β-arrestin cells gave a dose-dependent activation with an EC_{50} of 2.1×10^{-12} M (Fig. 4*H*). Notably, compound 43 was unable to activate the β-arrestin system stably expressing ADP receptor $P2Y_{12}$, indicating the selectivity of ligand GPCR interactions (Fig. S6). These results suggest that RvD1 interacts with both ALX and GPR32.

Expression of GPR32 and ALX in Human MΦ Regulates RvD1-Stimulated Phagocytosis. Because complete resolution of acute inflammation involves phagocytosis and clearance of apoptotic PMNs by MΦ from the inflammatory milieu, which is enhanced by resolvins (4), we investigated whether RvD1 can enhance the phagocytic activity of human MΦ. Human MΦ exposed to RvD1 following differentiation of peripheral blood monocytes enhanced their ability to ingest zymosan and apoptotic human

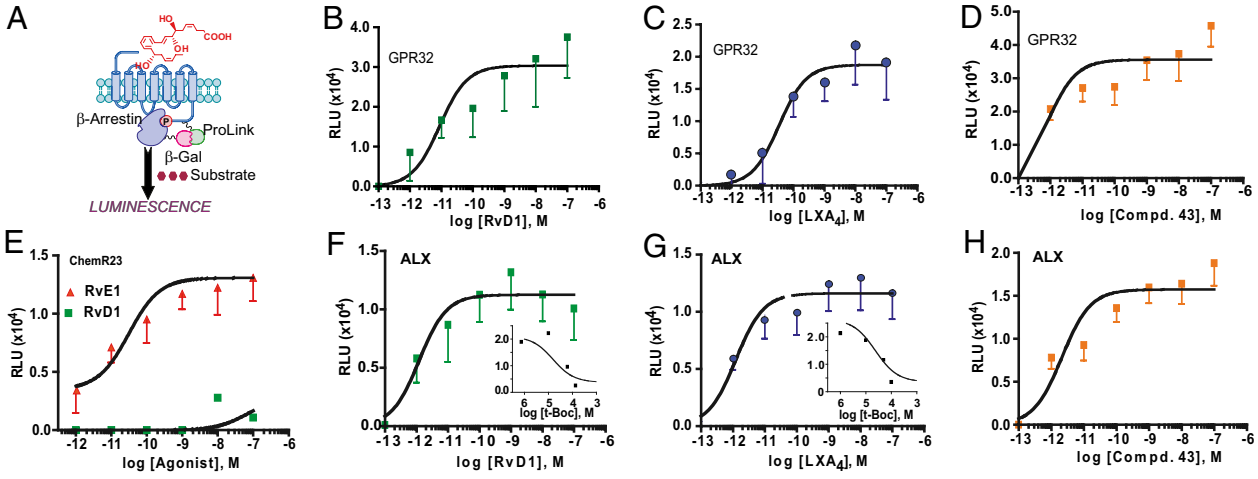

Fig. 4. RvD1 activates GPR32 and ALX receptors. (*A*) The β-arrestin system used to monitor receptor–ligand interaction (see text for details). (*B–D*) Dose responses obtained with RvD1, LXA_4, and compound (Compd) 43 with β-arrestin cells stably expressing GPR32. Results are mean ± SEM ($n = 4–8$). (*E*) RvE1 comparison with RvD1 with β-arrestin cells stably expressing the ChemR23 receptor; mean ± SEM ($n = 4$). (*F–H*) Dose responses obtained with RvD1, LXA_4, and compound 43 on β-arrestin cells stably expressing ALX; mean ± SEM ($n = 4–7$). (*Insets* in *F* and *G*) Concentration-dependent inhibition of ALX activation by RvD1 (*F*) and LXA_4 (*G*) in the presence of escalating concentrations of antagonist *t*-Boc-Met-Leu-Phe; means from triplicates of two separate experiments. (RLU, relative luminescence unit).

PMNs in a dose-dependent manner, which peaked at 1.0 and 0.1 nM (Fig. 5*A*) and was time-dependent (Fig. S7). Next, we transiently transfected human MΦ with expression vectors for the RvD1 candidate receptors, namely human GPR32 or ALX (Fig. 5 *B* and *C*, *insets*). RvD1 showed an increase in phagocytosis of zymosan particles in MΦ transfected with mock (Fig. 5*B*) that was further increased in MΦ overexpressing either GPR32 (Fig. 5*B*) or ALX (Fig. 5*C*). Conversely, MΦ with transient small hairpin RNA (shRNA) knockdown of ALX or GPR32 (Fig. 5 *D* and *E*) showed a decrease in RvD1-stimulated phagocytosis response (Fig. 5*F*). Although the knockdown of both GPCRs did not completely eliminate surface expression of each receptor, the RvD1 response was reduced and further decreased in MΦ with a double knockdown.

Discussion

Here, we demonstrated specific cell surface binding sites for RvD1, an endogenous anti-inflammatory and proresolving lipid mediator. The presence of RvD1 recognition sites on human phagocytes is of considerable interest in view of the potent actions of this autacoid (8, 12, 14). Two GPCRs that are denoted ALX, a lipoxin A_4 receptor, and an orphan, GPR32, were identified as directly interacting with RvD1. In addition, RvD1 regulates phagocytosis by human MΦ in a receptor-dependent manner. Together, these findings indicate that both ALX and GPR32 interact with RvD1 to signal its actions.

Resolution of inflammation is an active process with many control points, regulated by a unique genus of chemical mediators that are anti-inflammatory and proresolving (4, 9). Among these, RvD1 possesses potent actions demonstrable at the single-cell level with leukocytes in a microfluidics chamber (14). Nanomolar concentrations of RvD1 blocked actin polymerization in PMNs that were sensitive to inhibition by pertussis toxin, suggesting that the recognition sites belong to the family of GPCRs and most likely are coupled to G proteins of the Gi/o class. Screening systems used to assess PPAR activation indicated that neither RvD1 nor RvE1 directly activates PPAR signaling at concentrations that evoke anti-inflammatory responses (Fig. S3). Indeed, nuclear receptors belonging to the PPAR family have emerged as relevant in anti-inflammatory signaling mechanisms and may bind lipids (16). For example, oxidized fatty acids at concentrations in the micromolar range can activate PPARγ, which possesses an unusually large ligand-binding cavity that accommodates a wide range of molecules rather than a single ligand (21). Because RvD1 did not activate PPAR signaling within its bioactive concentration range, it was reasonable to determine whether the recognition sites were present on the surfaces of phagocytes, which was in line with the finding that RvD1 actions were PTX sensitive, pointing to the family of GPCRs.

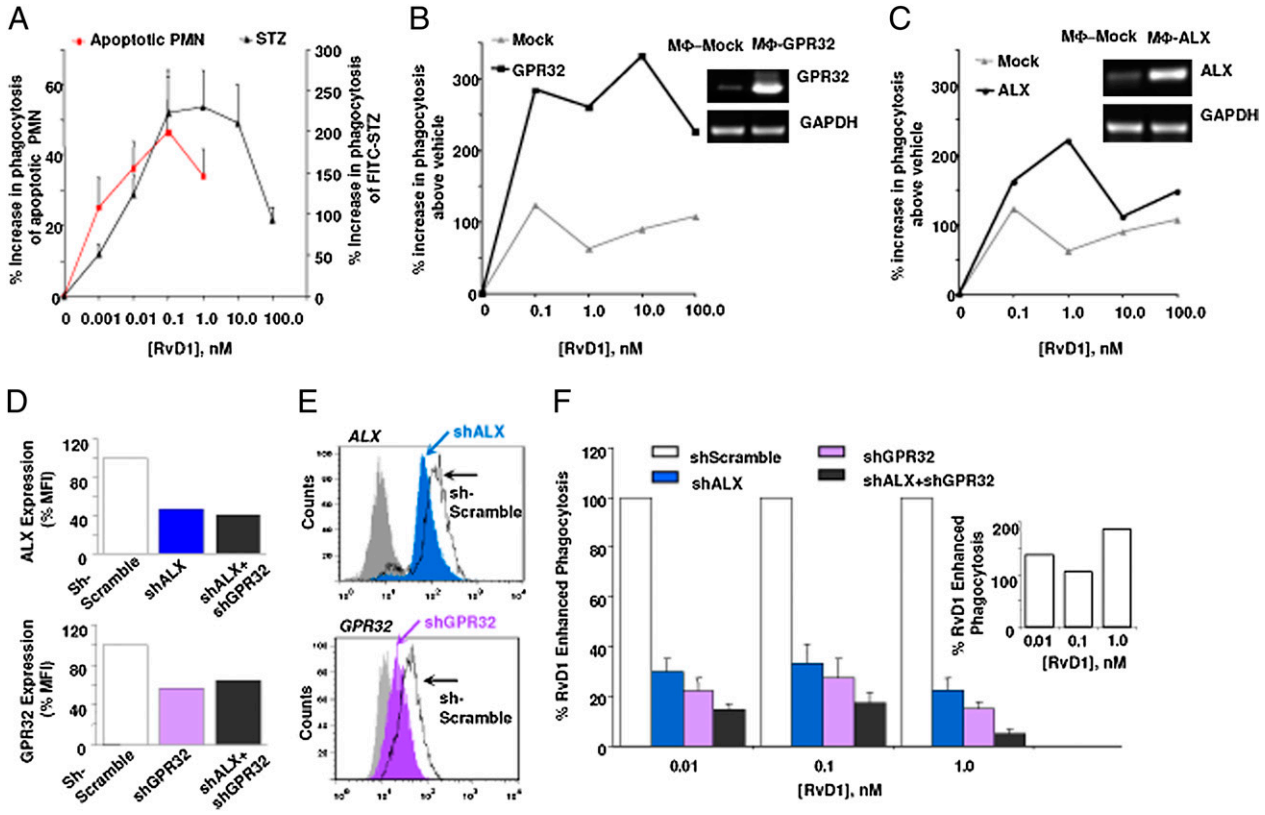

Fig. 5. RvD1 enhances human MΦ phagocytosis regulated by GPR32 and ALX. (*A*) RvD1 enhances MΦ phagocytosis of FITC–STZ and apoptotic human PMNs. Increases in phagocytosis were determined by monitoring total fluorescence from ingested FITC–STZ particles or apoptotic PMNs labeled with carboxyfluorescein diacetate-succinimidyl ester; mean ± SEM, $*P < 0.05$ vs. vehicle, $n = 5$ healthy subjects. (*B* and *C*) Overexpression of GPR32 (*B*) and ALX (*C*) in human MΦ increases RvD1-stimulated phagocytosis. Results are the percentage increase in phagocytosis and are representative of three healthy subjects in quadruplicates. (*Insets* in *B* and *C*) Expression of GPR32 (*B*) and ALX (*C*) mRNAs from MΦ transfected with cDNAs for the respective GPCRs. (*D–F*) shRNA knockdown of ALX, GPR32, or both reduces RvD1-enhanced phagocytosis. (*D*) Surface expression levels of ALX (*Upper*) and GPR32 (*Lower*) in single and double knockdown of GPCRs compared to sh scramble-transfected MΦ; representative of three healthy subjects. (*E*) Representative histograms from three healthy subjects showing ALX (*Upper*) and GPR32 (*Lower*) staining in shRNA-transfected MΦ. (*F*) Percentage RvD1-enhanced phagocytosis; comparison between sh scramble, shALX, shGPR32, and double knockdown MΦ; mean ± SEM of quadruplicate determinations from six healthy subjects. (*Inset*) Percentage of RvD1-enhanced phagocytosis in sh scramble-transfected MΦ.

[^{3}H]-RvD1 prepared by total organic synthesis was used to identify high-affinity cell-surface recognition sites for RvD1 on human leukocytes, giving a K_d of ~0.2 nM (~75 pg/mL), which is within the range of its levels measured in murine cells and tissues, i.e., >75–300 pg (13, 22), and bioactions. Of interest, LXA_4 partially displaced [^{3}H]-RvD1 specific binding to human PMNs. A screening system for identifying receptor candidates, which tests the ability of receptor–ligand coupling to counteract TNF-α-stimulated NF-κB activation (10), gave candidate GPCRs, namely ALX, a LXA_4 receptor (23), and an orphan, GPR32. GPR32 consists of 356 deduced amino acids and shares a sequence identity of 35–39% homology with members of the chemoattractant receptor family (24). Using a cDNA array, GPR32 mRNA expression was detected in PBLs and in arterial and venous tissues (Fig. S8*A*). Also, mRNA expression was identified by PCR in human myeloid cells (e.g., PMNs, monocytes, and MΦ) and in human umbilical vein endothelial cells (HUVEC) (Fig. S8*A*, *Inset*). Additionally, cell-surface expression of GPR32 was present on human PMNs, monocytes, and differentiated MΦ populations as determined by flow cytometry using an anti-GPR32 antibody (Fig S8*B*). Interestingly, GPR32 and ALX surface expressions in human monocytes were upregulated on exposure to GM-CSF and zymosan (Fig. S8*C*), but not by exposure to TNF-α or TGF-β (Fig. S8*D*). This correlates with RvD1 actions on macrophages that enhance clearance of zymosan particles.

RvD1 interactions with human ALX and GPR32 were further evaluated using another reporter system, one that monitors, in a ligand-dependent fashion, coupling of intracellular β-arrestin with GPCR cytoplasmic domains. This system permits monitoring of ligand–receptor interactions without classic second messengers involved (25). This was needed because RvD1 did not directly evoke Ca^{2+} mobilization nor changes in cAMP levels (Fig. 1). This system employed recombinant cells engineered to stably overexpress ALX, ChemR23, or GPR32, each tagged with the Pro-Link peptide of β-gal and β-arrestin linked to the enzyme acceptor (EA) fragment of β-gal. With this system, LXA_4 was also identified as interacting with GPR32, suggesting that this GPCR may be part of a cluster of receptors transducing proresolution signals with lipid mediators. Along these lines, an ALX agonist—denoted compound 43 and recently identified via a medicinal chemistry screen with anti-inflammatory actions in vivo (19)—also activates both ALX and GPR32 in stable β-arrestin cell systems. The β-arrestin signal in this system activated by agonists showed a more than twofold increase compared to the vehicle, which is in agreement with signal-to-noise ratios obtained for other receptors for lipid mediators, e.g., prostanoid receptors with their respective ligands (26). Transient transfection of human MΦ with expression vector for either ALX or GPR32 increased the ability of RvD1 to enhance phagocytosis, suggesting that the RvD1 response is both ALX- and GPR32-dependent. Moreover, shRNA knockdown of these GPCRs in human MΦ reduced RvD1-stimulated phagocytosis. These findings functionally validate results from the reporter systems used to identify ALX and GPR32 as interacting with RvD1.

Proresolving lipid mediators exert their actions by interacting with GPCRs with high affinity and stereospecificity. For example, RvE1 binds both ChemR23 and BLT1 and LXA_4 binds ALX/FPR2 (5, 10, 11). Interestingly, these ligands bind to more than one receptor to mediate their actions, which in most cases are cell-type-specific. RvE1 stimulates proresolution pathways via ChemR23, which is abundantly expressed in MΦ and dendritic cells (10), whereas it binds to BLT1 for its anti-PMN actions (11). Along these lines, ChemR23 knockout mice are unable to resolve zymosan-induced peritonitis in the presence of C-15, a peptide ligand for this receptor, indicating proresolving signaling by this receptor (27). In the present report, we identified two receptors that specifically interact with RvD1, namely ALX and GPR32. NCBI blast analysis for murine orthologs of human GPR32 did not reveal apparent candidates with significant sequence homology. An ortholog for human GPR32 was identified in the chimpanzee (*Pan troglodytes*; see the NCBI database at www.ncbi.nlm.nih.gov), but is absent in the dog genome and is a pseudogene in the rat and mouse (28). The murine counterparts of human GPR32 remain unknown. Also, heterodimerization of eicosanoid GPCRs, e.g., PGI_2 receptor (IP) and thromboxane A_2 receptor (TPα) (29), is known. Hence, it is possible that resolvins could signal via heterodimeric GPCRs. However, with the current reagents, we were not able to obtain evidence for RvD1-dependent heterodimerization of ALX with GPR32. Also, this does not preclude either ALX or GPR32 interacting with other GPCRs when RvD1 is present.

LXA_4 and RvD1 share some anti-inflammatory and proresolving actions in human and murine systems (9, 12, 30, 31), yet each is biosynthesized at different time intervals during resolution and via distinct biosynthetic routes (4). In summary, RvD1 specifically binds to human phagocytes and activates two separate GPCRs, namely ALX and GPR32. RvD1 enhances the phagocytic and clearance functions of human MΦ, which were increased by these GPCRs. Taken together, these findings suggest that RvD1 executes its proresolving actions within human tissues via its interactions with ALX and GPR32.

Materials and Methods

[^{3}H]-RvD1 Binding. Fresh human PMNs were isolated by dextran–Histopaque double gradient from whole blood from healthy volunteers (deidentified) who denied taking medications 2 weeks before donation (Brigham and Women's Hospital protocol no. 88–02642). Specific binding with PMNs was performed essentially as in ref. 31. PMNs were suspended in PBS with $CaCl_2$ and $MgCl_2$ (pH 7.4). For saturation binding, aliquots of cells (5×10^6) were incubated with increasing concentrations of freshly isolated [^{3}H]-RvD1 in the presence or absence of 10 μM of unlabeled RvD1 (1 h at 4°C). Competition binding was assessed by incubating aliquots (5×10^6 cells) with 10 nM of [^{3}H]-RvD1 with or without 10 μM heteroligands (1 h at 4°C). Bound and unbound radioligands were separated by filtration, and radioactivity was determined. Binding curves and Scatchard plots were constructed and K_d values were calculated using Prism software.

Actin Polymerization and CD11b Surface Expression. Fresh human PMNs were incubated with 1 μg/mL of either PTX or activated cholera toxin for 2 h at 37°C, followed by either RvD1 (10 nM) or a vehicle (15 min). Cells were permeabilized and stained with FITC–phalloidin for FACS (Becton Dickinson and CellQuest). RvD1 regulation of LTB_4-stimulated actin polymerization was assessed with human PMNs with additions of RvD1 (10 nM, 15 min at 37°C) followed by LTB_4 (10 nM), actin staining and FACS. PMN CD11b surface expression was assessed as in ref. 32.

Intracellular Ca^{2+} Mobilization. Ca^{2+} levels in human PMNs were determined using a Flexstation III plate reader (Molecular Devices). Cells were loaded with Fura-2 AM and plated (0.5×10^6/well; 96-well), and RvD1 or LTB_4 was added at 60 s, emitted fluorescence was recorded, and the magnitude of the calcium response was calculated, i.e., the ratio of fluorescence intensity of ion-bound (λ 380 nm) and ion-free forms (λ 340 nm).

GPCR cDNA Cloning and NF-κB Reporter Gene Expression. Full-length encoding cDNAs for GPCR–ALX (P25090), FPR (P21462), ChemR23 (Q99788), GPR1 (A55733), GPR32 (O75388), CB1 (P47746), BLT_1 (Q15722), and BLT_2 (Q9JJL9) were cloned into pcDNA3 vector by RT–PCR using primers designed according to the GenBank/EMBL/DDBJ database. HeLa cells (75,000 cells/well) were transiently transfected with 100 ng pNF-κB luciferase (Stratagene), 800 ng of either pcDNA3 or pcDNA3–GPCRs, and internal standard pRL-TK (Promega) using Lipofectamine 2000. After 24 h, cells were exposed to RvD1 (10 nM) or a vehicle for 30 min plus human TNF-α (1 ng, 6 h at 37 °C). Luciferase activity was measured by a dual-luciferase reporter system.

GPCR β-Arrestin System: RvD1 Receptor–Ligand Interactions. Cells were engineered to coexpress β-arrestin tagged with an inactive moiety of β-galactosidase EA protein together with a candidate GPCR fused to the Pro-Link peptide. The PathHunter system (DiscoveRx) uses enzyme fragment complementation (18) based on bioluminescence resonance energy transfer

to measure receptor–ligand interaction. In the presence of ligand, activated GPCR interacts with β-arrestin, bringing to proximity EA and Pro-Link fragments of β-gal, which forms a holoenzyme. Its activity was measured by generating a chemiluminescent signal (18). HEK and CHO cells were engineered to stably coexpress β-arrestin tagged with β-galactosidase EA and human ALX, GPR32, or ChemR23 (custom constructs), linked to the Pro-Link peptide. HEK-ALX, CHO-GPR32, and CHO-ChemR23 were grown in medium with selection antibiotics. Twenty-four hours before incubations, cells were plated in 96-well plates (20,000 or 10,000 cells/well) and then in serum-free medium (1h at 37 °C). Receptor activation was determined by chemiluminescence (PathHunther EFC detection kit) catalyzed by β-gal using a luminometer (EnVision, PerkinElmer).

Human MΦ and Phagocytosis. Monocytes were isolated from human whole blood using immunomagnetic selection with CD14 microbeads (Miltenyi Biotech) and cultured in RPMI with 10 ng/mL human GM–CSF (R&D Systems) at 37 °C for 7 days. For phagocytosis of serum-treated zymosan A (STZ), MΦ (0.1×10^6 cells/well in a 24-well plate) were exposed to RvD1 or a vehicle (15 min at 37 °C). FITC–STZ from *Saccharomyces cerevisiae* (Molecular Probes) was then added to cells (0.5×10^6 particles/well) and incubated (30 min at 37 °C) in the dark. Supernatants were aspirated, and trypan blue (0.03% in $PBS^{+/+}$ for ~60 s) was added to quench extracellular FITC–STZ. Fluorescence was measured using a Victor plate reader (PerkinElmer). For apoptotic PMNs, isolated human PMNs were labeled with carboxyfluorescein diacetate (10 μM, 30 min at 37 °C; Molecular Probes) and allowed to undergo apoptosis in RPMI plus 10% FBS (5×10^6 cells/mL) for 16–18 h. MΦ cells (0.1×10^6 cells/well) were incubated with RvD1 or a vehicle (15 min at 37 °C). Apoptotic PMNs were added at 1:5–1:10 (MΦ:PMN), with phagocytosis carried out at 37 °C for 60 min, and fluorescence was monitored with a Victor plate reader.

Transfection of Human MΦ. MΦ cells (5×10^6 cells) were transfected with pcDNA3 or with expression vectors for human ALX or GPR32 using a MΦ Jet-Pei transfection reagent. At 24 h post transfection, cells were transferred to 24-well plates (50,000 cells/well), and phagocytosis was carried out 48 h post adhesion as above. Transfection efficiency was assessed by PCR monitoring of receptor mRNA levels normalized to GAPDH. For GPCR knockdown, shRNA plasmids targeting ALX, GPR32, or scrambled shRNA (SA Biosciences) were transiently transfected into MΦ cells as above. Receptor knockdown was assessed by FACS.

Statistical Analysis. Data are presented as mean ± SEM. Statistical analysis was performed using the paired or unpaired Student's t test, and $P < 0.05$ was considered to be significant.

ACKNOWLEDGMENTS. We thank M. H. Small for expert assistance in manuscript preparation and Dr. Makoto Arita for the initial preparation of GPCR clones for screening. We also thank Drs. Lucy Norling and Gabrielle Fredman for help with leukocyte isolation and the Institute for Chemistry and Chemical Biology-Longwood, Harvard Medical School for use of their fluorescent plate reader. This study was supported in part by the National Institutes of Health Grants GM38765 (to C.N.S.), and P50-DE016191 (to C.N.S.).

1. Shimizu T (2009) Lipid mediators in health and disease: Enzymes and receptors as therapeutic targets for the regulation of immunity and inflammation. *Annu Rev Pharmacol Toxicol* 49:123–150.
2. Mantovani A, Allavena P, Sica A, Balkwill F (2008) Cancer-related inflammation. *Nature* 454:436–444.
3. Hansson GK, Robertson AK, Söderberg-Nauclér C (2006) Inflammation and atherosclerosis. *Annu Rev Pathol* 1:297–329.
4. Serhan CN (2007) Resolution phase of inflammation: Novel endogenous anti-inflammatory and proresolving lipid mediators and pathways. *Annu Rev Immunol* 25: 101–137.
5. Fiore S, Maddox JF, Perez HD, Serhan CN (1994) Identification of a human cDNA encoding a functional high affinity lipoxin A4 receptor. *J Exp Med* 180:253–260.
6. Maderna P, Godson C (2005) Taking insult from injury: Lipoxins and lipoxin receptor agonists and phagocytosis of apoptotic cells. *Prostaglandins Leukot Essent Fatty Acids* 73:179–187.
7. Calder PC (2007) Immunomodulation by omega-3 fatty acids. *Prostaglandins Leukot Essent Fatty Acids* 77:327–335.
8. Serhan CN, et al. (2002) Resolvins: A family of bioactive products of omega-3 fatty acid transformation circuits initiated by aspirin treatment that counter proinflammation signals. *J Exp Med* 196:1025–1037.
9. Serhan CN, Chiang N (2008) Endogenous pro-resolving and anti-inflammatory lipid mediators: a new pharmacologic genus. *Br J Pharmacol* 153 (Suppl 1):S200–S215.
10. Arita M, et al. (2005) Stereochemical assignment, antiinflammatory properties, and receptor for the omega-3 lipid mediator resolvin E1. *J Exp Med* 201:713–722.
11. Arita M, et al. (2007) Resolvin E1 selectively interacts with leukotriene B4 receptor BLT1 and ChemR23 to regulate inflammation. *J Immunol* 178:3912–3917.
12. Sun YP, et al. (2007) Resolvin D1 and its aspirin-triggered 17R epimer. Stereochemical assignments, anti-inflammatory properties, and enzymatic inactivation. *J Biol Chem* 282:9323–9334.
13. Merched AJ, Ko K, Gotlinger KH, Serhan CN, Chan L (2008) Atherosclerosis: Evidence for impairment of resolution of vascular inflammation governed by specific lipid mediators. *FASEB J* 22:3595–3606.
14. Kasuga K, et al. (2008) Rapid appearance of resolvin precursors in inflammatory exudates: Novel mechanisms in resolution. *J Immunol* 181:8677–8687.
15. Naccache PH, Faucher N, Therrien S, Borgeat P (1988) Calcium mobilization, actin polymerization and right-angle light scatter responses to leukotriene B4, 12(R)- and 12(S)-hydroxyeicosatetraenoic acid in human neutrophils. *Life Sci* 42:727–733.
16. Barish GD, et al. (2008) PPARdelta regulates multiple proinflammatory pathways to suppress atherosclerosis. *Proc Natl Acad Sci USA* 105:4271–4276.
17. Perretti M, D'Acquisto F (2009) Annexin A1 and glucocorticoids as effectors of the resolution of inflammation. *Nat Rev Immunol* 9:62–70.
18. Olson KR, Eglen RM (2007) Beta galactosidase complementation: A cell-based luminescent assay platform for drug discovery. *Assay Drug Dev Technol* 5:137–144.
19. Bürli RW, et al. (2006) Potent hFPRL1 (ALXR) agonists as potential anti-inflammatory agents. *Bioorg Med Chem Lett* 16:3713–3718.
20. Perretti M, Getting SJ, Solito E, Murphy PM, Gao JL (2001) Involvement of the receptor for formylated peptides in the in vivo anti-migratory actions of annexin 1 and its mimetics. *Am J Pathol* 158:1969–1973.
21. Itoh T, et al. (2008) Structural basis for the activation of PPARgamma by oxidized fatty acids. *Nat Struct Mol Biol* 15:924–931.
22. Duffield JS, et al. (2006) Resolvin D series and protectin D1 mitigate acute kidney injury. *J Immunol* 177:5902–5911.
23. Chiang N, et al. (2006) The lipoxin receptor ALX: Potent ligand-specific and stereoselective actions in vivo. *Pharmacol Rev* 58:463–487.
24. Marchese A, et al. (1998) Cloning genes encoding receptors related to chemoattractant receptors. *Genomics* 50:281–286.
25. Pierce KL, Premont RT, Lefkowitz RJ (2002) Seven-transmembrane receptors. *Nat Rev Mol Cell Biol* 3:639–650.
26. Fowler A, Wehrman T, Peng K, Bassoni D, Olsen K (2007) Development of a non-imaging, homogenous assay format for analysis of arrestin recruitment as a detection method for generic GPCR screening. *Proc Life Sci PC482* .
27. Cash JL, et al. (2008) Synthetic chemerin-derived peptides suppress inflammation through ChemR23. *J Exp Med* 205:767–775.
28. Haitina T, Fredriksson R, Foord SM, Schiöth HB, Gloriam DE (2009) The G protein-coupled receptor subset of the dog genome is more similar to that in humans than rodents. *BMC Genomics* 10:24.
29. Wilson SJ, Roche AM, Kostetskaia E, Smyth EM (2004) Dimerization of the human receptors for prostacyclin and thromboxane facilitates thromboxane receptor-mediated cAMP generation. *J Biol Chem* 279:53036–53047.
30. Patcha V, et al. (2004) Differential inside-out activation of beta2-integrins by leukotriene B4 and fMLP in human neutrophils. *Exp Cell Res* 300:308–319.
31. Chiang N, Fierro IM, Gronert K, Serhan CN (2000) Activation of lipoxin A(4) receptors by aspirin-triggered lipoxins and select peptides evokes ligand-specific responses in inflammation. *J Exp Med* 191:1197–1208.
32. Kishimoto TK, Jutila MA, Berg EL, Butcher EC (1989) Neutrophil Mac-1 and MEL-14 adhesion proteins inversely regulated by chemotactic factors. *Science* 245:1238–1241.
33. Okuno T, et al. (2008) 12(S)-Hydroxyheptadeca-5Z, 8E, 10E-trienoic acid is a natural ligand for leukotriene B4 receptor 2. *J Exp Med* 205:759–766.